

# The activity of the tetrahedral Au<sub>20</sub> cluster: charging and impurity effects

L.M. Molina<sup>a,\*</sup>, B. Hammer<sup>b</sup>

<sup>a</sup> Departamento de Física Teórica, Universidad de Valladolid, E-47011 Valladolid, Spain

<sup>b</sup> iNANO and Department of Physics and Astronomy, University of Aarhus, DK-8000 Aarhus C, Denmark

Received 26 February 2005; revised 25 April 2005; accepted 28 April 2005

Available online 13 June 2005

## Abstract

Several issues concerning the activity of the magical Au<sub>20</sub> cluster are addressed with the help of Density Functional Theory (DFT) simulations. First, the cluster is found to be extremely robust against distortions when supported at an oxide (MgO) surface, keeping its tetrahedral shape. Second, the activity toward CO oxidation is studied as a function of the cluster charge state. Whereas the neutral cluster is found to be only moderately active, the anion becomes extremely active, because of the presence of a weakly bound unpaired electron. The attempt to induce cluster charging upon attachment to a charged surface F<sup>+</sup>-center was unsuccessful, with a cluster only slightly more active than the unsupported, neutral one. Finally, some initial steps towards the rational design of active catalysts were taken by the study of the effect of having different impurities. Promising results are obtained by the addition of an extra Na atom, which preferentially adsorbs inside the tetrahedron. Two competing isomers with an endohedral Na atom within a Au<sub>20</sub> cage are found, and both of them are very active.

© 2005 Elsevier Inc. All rights reserved.

**Keywords:** Gold; Clusters; Surfaces; CO; Oxidation; DFT; Promoters

## 1. Introduction

Small Au nanoparticles supported at metal oxides are currently receiving a lot of attention because of their surprising catalytic properties [1–3]. Moreover, in order to clarify the origin of that activity (and the reaction mechanisms), much research has been devoted to the catalytic activity of small Au clusters containing few ( $\approx 1$ –20) Au atoms, where some important parameters such as size and charge state can be controlled. Both soft-landing of size-selected clusters [4–7] and either experimental [8–11] or theoretical [12–18] studies of gas-phase clusters have been used to obtain some understanding of the catalysts' features at the molecular level, focusing on the low temperature CO oxidation reaction.

In the ongoing discussion, there is ample evidence that free neutral clusters with high HOMO-LUMO gaps are very active as anions, because of their small electronic affinity, which favors electron transfer to a strongly bound molecu-

lar O<sub>2</sub>. One particular example is Au<sub>6</sub><sup>−</sup>, which was recently identified as highly active for the CO + O<sub>2</sub> reaction [9]. Another interesting case is the Au<sub>20</sub> cluster. Very recently, this cluster was identified as particularly stable, with a large HOMO-LUMO gap of 1.77 eV due to both a magic number of valence electrons (20, corresponding to one of the shell closings of the jellium model) and a very compact, close-packed tetrahedral shape [19]. These facts suggest that binding of O<sub>2</sub> to the Au<sub>20</sub><sup>−</sup> anion will be strong, possibly rendering the cluster very reactive. Further interest in this cluster has arisen very recently because of its solution synthesis (protected by PPh<sub>3</sub> ligands), achieved by Zhang and co-workers [20].

However, despite the interest in these results for free charged clusters, other important considerations must be taken into account for a discussion of the activity of catalysts to be used in practical applications, which are generally neutral and supported. When supported, clusters are likely to distort and possibly undergo fundamental structural changes. Furthermore, the cluster–support interaction can also change the electronic structure of the cluster, altering its reactiv-

\* Corresponding author. Fax: +34 983 423013.

E-mail address: [lmolina@fta.uva.es](mailto:lmolina@fta.uva.es) (L.M. Molina).

ity [21–23]. Experiments involving soft-landing of small Au clusters on an MgO surface suggest an important role of electron-rich surface defects (F-centers), which can enhance the cluster's reactivity by transferring charge to them [4,5]. In this paper we deal with several issues related to the reactivity of the “magical” Au<sub>20</sub> tetrahedral cluster toward CO oxidation and to its possible use in practical applications.

First, we studied the stability of the tetrahedral shape for the supported cluster. Choosing MgO(100) as a support, we compared the stabilities of several Au<sub>20</sub> isomers supported at both perfect and defective (F<sup>+</sup>-center) MgO and found in both cases the tetrahedral shape to be fairly robust and likely to survive upon soft-landing. Second, we studied the binding of CO and O<sub>2</sub> to unsupported (both neutral and negatively charged) Au<sub>20</sub> and to the cluster supported at either perfect or defective MgO(100). The free neutral cluster was found to be only moderately active, with nearly unchanged activity for the cluster supported at perfect MgO(100). As should be expected, the cluster is very active as a free anion, but attaching the neutral cluster to an F<sup>+</sup>-center (composed of an electron residing in the surroundings of a missing O<sup>2-</sup>-anion) only weakly enhances reactivity over that of the neutral free cluster. Our results indicate that this extra electron is strongly pinned by the Madelung potential of the oxide. Third, since binding of the cluster to an electron-rich defect does not seem to significantly activate the cluster, we explored the possibility of enhancing the reactivity by adding a dopant to it. It was shown recently that Sr addition to small Au clusters results in much larger activities [5]. This is due to a facile electron transfer from the dopant to adsorbing O<sub>2</sub>. Choosing various alkali atoms as dopants (with the purpose of donating one extra electron, thus attaining an electronic configuration similar to the one of Au<sub>20</sub><sup>-</sup>), we found sodium to be particularly promising; a single Na atom was preferentially incorporated inside the tetrahedral “cage,” with a large activity enhancement. Finally, another competing isomer of Na<sub>1</sub>Au<sub>20</sub> was found, also based on Na located inside a Au cage, being exceptionally active for CO oxidation as well.

## 2. Theoretical basis

The simulations were performed with the DACAPO code [24], which uses a plane-wave basis set [25] (expanded up to 25 Ry), ultra-soft pseudopotentials [26] (a scalar-relativistic one, in the case of Au), and the gradient-corrected PW91 functional [27] for exchange-correlation effects. Spin-orbit coupling is not included, since it has recently been shown that it does not alter the relative stability between isomers and has only a small effect on HOMO–LUMO gaps [28]. For the simulations involving unsupported clusters, a large unit cell was used, separating the clusters in neighboring cells by at least 8 Å. For supported clusters, a frozen 2-layer-thick slab in a *p*(5 × 5) surface unit cell was used, from which a neutral surface oxygen atom was removed to cre-

ate an F-center. We simulated the F<sup>+</sup>-center by replacing the substrate Mg cation just below the vacancy with a Na cation, which effectively reduced the amount of charge concentrated in the vacancy from two electrons to one. In all cases, because of the large unit cells used, only one *k*-point (Γ) was used for the *k*-point sampling, because it provides a reasonably good convergence. Test calculations for smaller clusters show that neither relaxation of the substrate nor the use of thicker slabs significantly modified the energetics. The Au<sub>20</sub> and Na<sub>1</sub>Au<sub>20</sub> clusters and any adsorbates on them were fully relaxed.

## 3. Results

In Fig. 1 we show the relaxed structures (at the stoichiometric surface) of several supported Au<sub>20</sub> isomers, including the tetrahedron. The isomers were constructed based on reasonable arguments related to close-packing and maximization of cluster–support interaction. Moreover, a planar isomer (h) was included in the comparison, since planar isomers, because of relativistic effects [29], are found to compete with 3D structures up to quite large sizes (≈12 atoms) [30]. The presence of an F<sup>+</sup>-center results in a downward distortion of the Au atom placed on top of the vacancy, without a severe overall cluster distortion (compare Fig. 1a1 with 1a2). The relative stabilities are listed in Table 1. The tetrahedral shape is more stable (by 2–3 eV) than any other shape for the unsupported cluster, and even if some isomers show stronger adhesion to the support, this is never able to compensate for the energetic cost of distorting the tetrahedral structure. This happens for both perfect and defective surfaces, although in the latter case the effect is more pro-

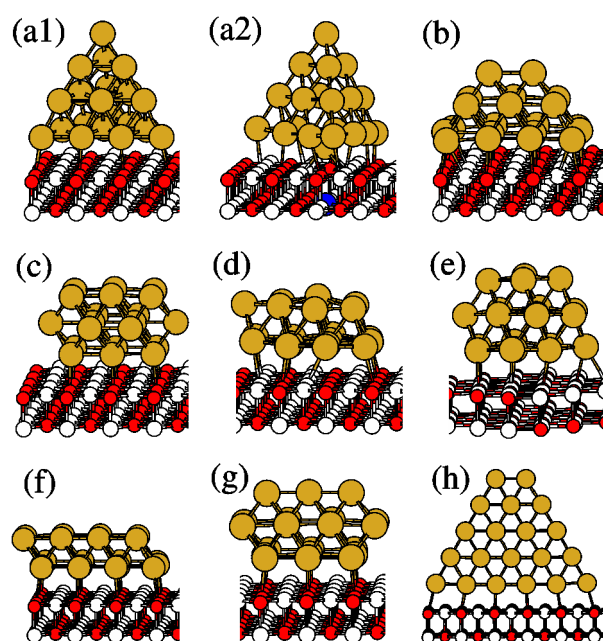


Fig. 1. Structure of several Au<sub>20</sub> isomers supported at the perfect MgO(100) surface (an F<sup>+</sup>-center, for (a2)).

Table 1

Energy differences (relative to the most stable tetrahedral isomer) for clusters both unsupported ( $\Delta E_{\text{uns}}$ ) and supported ( $\Delta E_{\text{sup}}$ ) at either a perfect MgO(100) surface or at an  $F^+$ -center. On either case, also adhesion energies  $E_{\text{adh}}$  are provided. The labels for the different isomers correspond to the various panels of Fig. 1. All quantities in eV

	Isomer							
	a	b	c	d	e	f	g	h
Perfect MgO support								
$\Delta E_{\text{uns}}$	0.0	2.70	2.90	1.76	1.66	3.33	2.89	2.08
$\Delta E_{\text{sup}}$	0.0	1.16	2.40	2.01	2.10	2.37	1.65	1.47
$E_{\text{adh}}$	1.97	3.51	2.48	1.71	1.53	2.93	3.21	2.57
$F^+$ -center								
$\Delta E_{\text{sup}}$	0.0	0.20	1.79	1.71	1.48	1.46	0.87	1.06
$E_{\text{adh}}$	3.44	5.94	4.54	3.48	3.62	5.31	5.46	4.46

Table 2

Binding energies (in eV) of CO and O<sub>2</sub> to (a) free neutral Au<sub>20</sub>, (b) free Au<sub>20</sub><sup>−</sup>, (c) Au<sub>20</sub>/MgO(perfect), (d) Au<sub>20</sub>/F<sup>+</sup>-center, (e) Au<sub>20</sub>/F-center and (f) free neutral Na<sub>1</sub>Au<sub>20</sub>

Configuration	(a)	(b)	(c)	(d)	(e)	(f)
CO-apex	0.84	1.21	0.83	0.92	0.79	1.05
CO-edge	0.54	0.56	0.54	0.49	0.60	0.45
CO-facet	0.38	0.36	0.38	0.16	0.20	0.65
O <sub>2</sub> -apex	0.15	1.14	0.22	0.36	0.26	0.53
O <sub>2</sub> -edge-edge <sup>a</sup>	0.0	0.78	0.0	0.05	0.04	0.01
O <sub>2</sub> -facet-edge <sup>a</sup>	0.0	0.34	0.0	0.0	0.0	0.36

<sup>a</sup> O<sub>2</sub>-edge-edge and O<sub>2</sub>-facet-edge represent configurations where O<sub>2</sub> bridges two Au atoms.

nounced and the overall stabilities are more similar. Therefore, the results suggest that the tetrahedral isomer is fairly robust and is likely to survive when it is soft-landed on MgO.

Next, we focus on the activity of Au<sub>20</sub> toward CO oxidation. Table 2 summarizes the binding energy of the reactants (CO and O<sub>2</sub>) to tetrahedral Au<sub>20</sub> in various situations: free Au<sub>20</sub> (either neutral or anion) and supported Au<sub>20</sub> (either stoichiometric MgO, F and F<sup>+</sup>-centers). Three binding configurations were considered in each case, and the three inequivalent sites of Au<sub>20</sub>, apex, edge, and facet atoms were explored. In agreement with the closed-shell character of neutral Au<sub>20</sub>, binding of O<sub>2</sub> is not feasible unless the cluster becomes negatively charged. In such a case, the cluster becomes very active, as one would expect, given the low electron affinity of the neutral cluster (2.15 eV). The preferred binding sites are clearly the corner atoms; this is mainly due to the fact that the electron populating the HOMO of Au<sub>20</sub><sup>−</sup> (i.e., the LUMO of Au<sub>20</sub>) is strongly localized at those sites (see Fig. 2). Strong activity changes are found as well for CO binding, with the binding energy correlating with the coordination of the binding site [31,32]. It is worth noting that charging of Au<sub>20</sub> enhances CO binding as well.

For the supported cluster, in the case of a perfect MgO (100) surface, because of the relatively weak character of the cluster–oxide interaction, the binding of both CO and O<sub>2</sub> closely resembles the result obtained for the unsupported

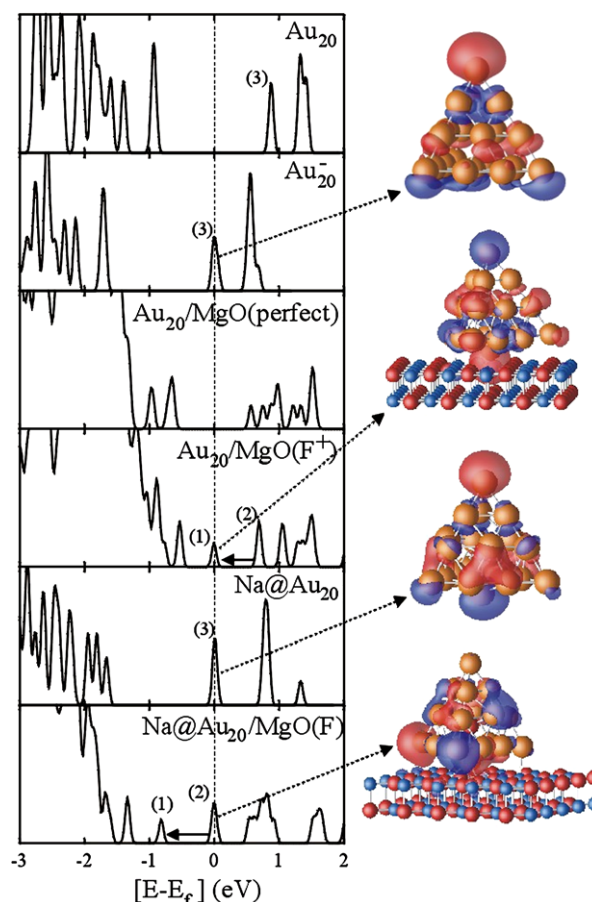


Fig. 2. Densities of states (DOS) around the Fermi level for Au<sub>20</sub> and Na<sub>1</sub>Au<sub>20</sub> on several different environments. Labels indicate degeneracies of electronic levels. To the right, isosurface plots of the real part of one of the HOMO levels of Au<sub>20</sub><sup>−</sup>, Au<sub>20</sub> supported at an MgO F<sup>+</sup>-center, and free and F-center supported Na<sub>1</sub>Au<sub>20</sub>-Td.

neutral cluster. This is no surprise, since the electronic structures of the free and supported clusters are very similar; in Fig. 2 it can be seen that the 1.78 eV HOMO–LUMO gap of the free cluster is only weakly modified by the cluster–support interaction. Overall, the cluster is found to be only moderately active; the main contribution comes from the upper corner site, which binds CO effectively. Placing the cluster at either an F or an F<sup>+</sup>-center has very little effect on the O<sub>2</sub> binding energy, despite the charged nature of the defect. This is due to some fundamental differences with respect to the free anion; for Au<sub>20</sub><sup>−</sup> the extra electron occupies one of the three degenerated HOMO levels of neutral Au<sub>20</sub>, which are strongly localized at the apex atoms. Localization in that region and at an orbital energetically much above the rest of Au valence electrons makes its transfer to one of the 2π\* orbitals of O<sub>2</sub> very easy. Consequently, O<sub>2</sub> binds strongly to the apex atoms. In contrast, for Au<sub>20</sub> supported at the F<sup>+</sup>-center, that electron is mostly localized around the Au atom on top of the defect (see Fig. 2, fourth panel) in a state shifted down in energy toward the valence band. Such electron trapping at the defect, where the electron is “pinned” by the Madelung potential of the oxide, makes charge transfer

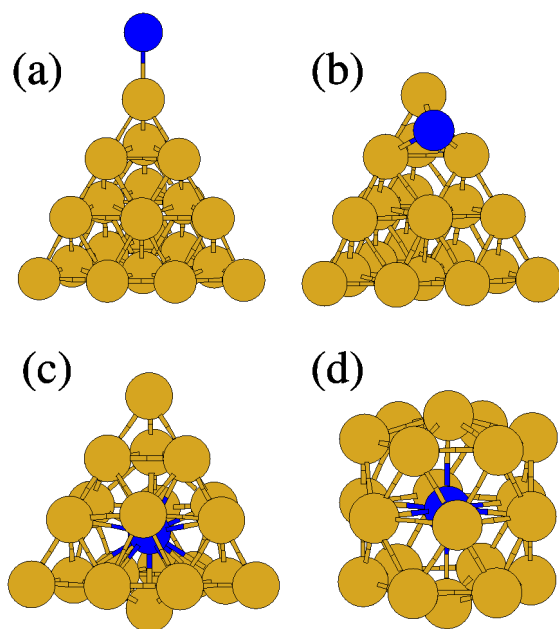


Fig. 3. Low energy isomers for the  $\text{Na}_1\text{Au}_{20}$  cluster.

Table 3

Relative energies (in eV) of various isomers of the alkali- $\text{Au}_{20}$  cluster; in the case of Na, also the stabilities of the cation are reported. The labels represent the different isomers in Fig. 3

Dopant	(a)	(b)	(c)	(d)
H	0.0	0.42	0.85	–
Li	0.08	0.0	0.41	–
Na	0.90	0.49	0.0	0.52
Na (cation)	–	0.63	0.59	0.0
K	–	0.0	1.39	0.98

to  $\text{O}_2$  more difficult, as the relatively weak binding of  $\text{O}_2$ , reduced bond length (1.27 Å), and high magnetic moment ( $1.5\mu_B$ ) further show.

We now study the addition of monovalent atoms to  $\text{Au}_{20}$ , and try to find a stable neutral cluster with an electronic structure analogous to the one of the very reactive  $\text{Au}_{20}^-$ . Here it must be noted that the special  $T_d$  geometry of  $\text{Au}_{20}$  makes it worthwhile to consider structures with an endohedral dopant, since  $\text{Au}_{20}$  lacks a core atom ( $\text{Au}_{20}$  can be viewed as the largest closed-packed metal cluster with every atom on the surface), and there is a small, empty space at the center of mass, separated by 1.7 Å from the closest atoms (facet atoms). From the point of view of catalyst design, this would lead to a substantial advantage, because of a larger resistance to degradation of the endohedral catalyst: a relatively weakly bound dopant at an exohedral location is much more likely to be evaporated by the heat release of the reaction (in the case of CO oxidation, around 3 eV for each  $\text{CO}_2$  molecule formed).

The structures for the most relevant isomers (in the case of Na) are shown in Fig. 3, and the relative energies are listed in Table 3. Na is found to be the most interesting dopant, since it clearly prefers to be located at an endohedral posi-

tion [33].<sup>1</sup> The presence of Na results in a sizable outward distortion of the “facet” Au atoms, by around 1 Å. For H and Li, the larger covalence of alkali-Au bonding makes exterior sites the preferred location, whereas for K the dopant is too large to fit inside the tetrahedron (for Cs, the endohedral location is not even metastable). Of course, in addition to a study of the preferred location of the dopant around the  $\text{Au}_{20}$  tetrahedron (isomers a–c), the possibility of Na doping altering the tetrahedral shape of the cluster must be checked. Relaxing a number of different close-packed isomers, we find that only the structure shown in Fig. 3d competes with the endohedrally doped tetrahedron (labeled from now on as  $\text{Na}_1\text{Au}_{20}\text{-T}_d$ ), because it is even more stable than the  $\text{Na}_1\text{Au}_{20}\text{-T}_d$  isomer for the cationic cluster. This structure consists of a roughly spherical  $\text{Au}_{20}$  cage with a Na atom at the center; (Johansson et al. have also reported highly stable cage-like structures for Au clusters [34]). The interest in the properties of the cation arises from the possibility of synthesizing the cluster through mass selection (maybe with posterior soft-landing upon a suitable substrate as MgO), a procedure that involves charged clusters. If we take into account the fact that a positively charged  $\text{Na}_1\text{Au}_{20}$  contains the magical number of 20 electrons, and its highly symmetrical and compact shape, a high abundance in the cluster beam should be expected.

The addition of endohedral Na dramatically improves the reactivity of the neutral  $\text{Au}_{20}$  cluster. For the  $\text{Na}_1\text{Au}_{20}\text{-T}_d$  isomer, both CO and  $\text{O}_2$  binding energies are systematically enhanced (see Table 2). The electronic structure of this cluster (see Fig. 2) closely resembles that of  $\text{Au}_{20}^-$ ; there are, however, some important differences, related to the distribution of the HOMO level, which is now shared between apex and facet sites. The latter become very active, even more than the edge sites. The other competing isomer,  $\text{Na}_1\text{Au}_{20}\text{-cage}$ , is also very active, with CO binding energies of 0.91, 0.62, and 0.57 eV at each of its three inequivalent sites, and  $\text{O}_2$  binding energies of 0.59 and 0.52 eV at the two most favorable binding configurations.

To further check on this activity enhancement, we have compared the activity of  $\text{Au}_{20}$ ,  $\text{Na}_1\text{Au}_{20}\text{-T}_d$  and  $\text{Na}_1\text{Au}_{20}\text{-cage}$ , modeling the reaction between coadsorbed CO and  $\text{O}_2$ . Before we comment on the results, shown in Fig. 4, it must be noted that the real environment where the reaction will take place should involve a relatively high concentration of adsorbed CO molecules. For free anions, Wallace and Whetten [35] have found multiply bonded CO with large saturation coverages, and Zhai and Wang have recently reported that the amount of adsorbed CO correlates with the number of available low-coordination sites [36]. Therefore, we first checked how high the CO concentration can be and the possibility of CO bonding at sites other than the most reactive ones.

<sup>1</sup> The preference of sodium for an endohedral location agree with the results obtained for Na doping of large Au nanoparticles, where a clear tendency for Na atoms to sink into a Au particle is found.



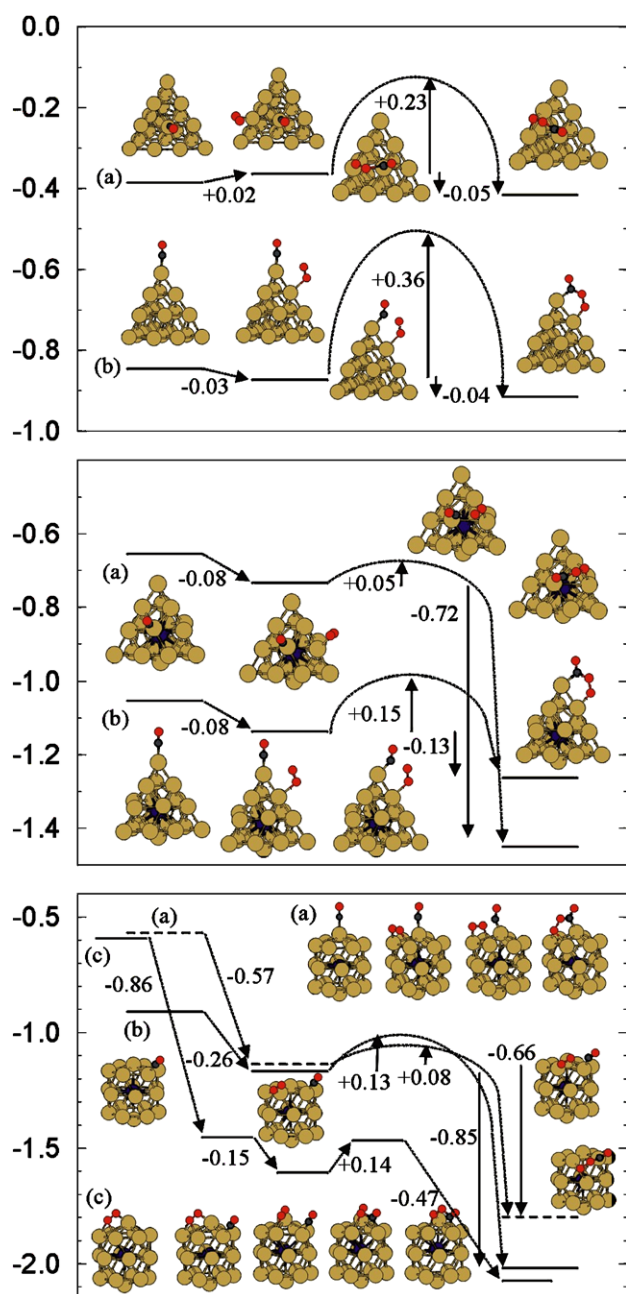


Fig. 4. Potential energy diagrams for the CO + O<sub>2</sub> reaction at neutral Au<sub>20</sub> (upper panel), Na<sub>1</sub>Au<sub>20</sub>-T<sub>d</sub> (middle panel) and Na<sub>1</sub>Au<sub>20</sub>-cage (lower panel). Several possible paths are shown in each case. All quantities in eV. The energy zero is set at cluster + CO(gas) + O<sub>2</sub>(gas) on each case.

The results are listed in Table 4, which compares the total CO binding energies with Au<sub>20</sub> and Na<sub>1</sub>Au<sub>20</sub>-T<sub>d</sub>. The table includes the total binding energies calculated with several CO present at the same time and the estimate based on Table 2 of the total binding energy of the CO's if they were noninteracting. On Au<sub>20</sub> a small CO attraction at high coverages is found, whereas on Na<sub>1</sub>Au<sub>20</sub>-T<sub>d</sub> a small repulsion is calculated. Overall the binding energies reveal that at around room temperature, all of the apex sites are expected to be covered by CO, and, in the case of Na<sub>1</sub>Au<sub>20</sub>-T<sub>d</sub>, CO can fur-

Table 4

Total CO binding energies  $E_b(\text{tot})$  and the corresponding estimations of the sum of binding energies  $\sum E_b$  assuming independent CO adsorption, for multiple CO adsorption at Au<sub>20</sub> and Na<sub>1</sub>Au<sub>20</sub>-T<sub>d</sub>. The labels indicate how many sites are occupied by CO, and their character (a = apex, f = facet). All quantities in eV

Au <sub>20</sub>	aa	af	ff	aaa	aaaa	aaaaf	aaaaff
$E_b(\text{tot})$	1.78	1.27	0.74	2.75	3.75	4.12	4.50
$\sum E_b$	1.69	1.23	0.77	2.53	3.38	3.76	4.15
$E_b(\text{tot})$	2.04	1.65	1.31	2.98	3.95	4.53	5.14
$\sum E_b$	2.11	1.71	1.31	3.16	4.21	4.87	5.52

ther adsorb at the active facet sites. This has some interesting implications, with respect to the recent synthesis of ligand-protected Au<sub>20</sub> by Zhang and co-workers [20]; since these authors have shown that ligands preferentially attach to the apex sites, thus blocking them, the presence of extra reactive sites becomes very important.

The potential energy diagrams in the upper two panels of Fig. 4 compare two analogous reaction paths (with CO initially bonded to either apex or facet sites) for Au<sub>20</sub> and Na<sub>1</sub>Au<sub>20</sub>-T<sub>d</sub>. These pathways start from CO and O<sub>2</sub> co-adsorbed at two neighboring sites and formation of a CO·O<sub>2</sub> intermediate complex, quite labile, which easily dissociates into CO<sub>2</sub> and adsorbed O [32] (we have checked, in the case of Na<sub>1</sub>Au<sub>20</sub>-T<sub>d</sub>, that direct O<sub>2</sub> dissociation is very unlikely, with high (1.5 eV) activation barriers and a very unstable final state). The comparison confirms the beneficial effect of Na doping: not only do the adsorbates bind more strongly to Na<sub>1</sub>Au<sub>20</sub>-T<sub>d</sub>; the activation barriers are also substantially reduced. Moreover, the energy gained as the final CO·O<sub>2</sub> complex is reached increases. The Na<sub>1</sub>Au<sub>20</sub>-cage isomer is even more active than Na<sub>1</sub>Au<sub>20</sub>-T<sub>d</sub>. In this case, new pathways (a, c) where CO reacts with a strongly bound O<sub>2</sub> can be considered; in both cases, very small (0.13 and 0.14 eV) activation barriers lead to the formation of a very stable CO·O<sub>2</sub> intermediate.

Finally, we have determined that, being supported at an MgO F-center, the Na<sub>1</sub>Au<sub>20</sub>-T<sub>d</sub> cluster<sup>2</sup> largely retains its gas-phase activity. However, the presence of the vacancy induces some interesting changes: the binding energy of O<sub>2</sub> at the topmost apex atom is only 0.38 eV (compared with 0.53 eV for the free cluster), whereas at the interfacial apex atoms it is enhanced to 0.66 eV; this asymmetry can be understood in terms of the electronic structure of the supported cluster, shown in Fig. 2. In the same way as for Au<sub>20</sub>, the vacancy electrons are pinned in the level labeled (1), which is localized mainly at the vacancy (with some small contribution at the topmost apex atom). Then, the additional electron provided by Na is shared among the remaining two Au<sub>20</sub> LUMO levels, localized (due to symmetry) at the interfacial apex atoms (see the eigenvalue plot in Fig. 2).

<sup>2</sup> Supported at an MgO F-center, the T<sub>d</sub> isomer is 0.47 eV more stable than the cage one (roughly the same energy difference as for the free neutral clusters).

#### 4. Conclusions

We can conclude that, for the important charge donation effect, it seems a more viable path to add to Au<sub>20</sub> a dopant such as Na rather than to rely on the excess charge at F or F<sup>+</sup> centers to provide the anionic behavior for the supported cluster. Moreover, given the tendency of Na to embed inside of Au clusters, the synthesis of these type of doped clusters may be feasible, with isolated Na atoms becoming seeds and, in the process of cluster growth, being surrounded by Au atoms until they are completely encapsulated. Then, magic clusters such as the two different isomers of Na<sub>1</sub>Au<sub>20</sub> studied may become, after mass selection and soft-landing, very interesting model catalysts.

#### Acknowledgments

This work was supported by the Danish Research Councils and the computational facilities of the Dansk Center for Scientific Computing. L.M.M. acknowledges the Spanish Ministry of Science and Technology for supporting his work through the Ramon y Cajal program, and support from the MCYT (MAT2002-04499) grant.

#### References

- [1] M. Haruta, *Catal. Today* 36 (1997) 153.
- [2] R. Meyer, C. Lemire, S.K. Shaikhutdinov, H.-J. Freund, *Gold Bull.* 37 (2004) 72.
- [3] P. Pyykkö, *Angew. Chem. Int. Ed.* 43 (2004) 4412.
- [4] A. Sanchez, W. Abbet, U. Heiz, W.D. Schneider, H. Häkkinen, R.N. Barnett, U. Landman, *J. Phys. Chem. A* 103 (1999) 9573.
- [5] H. Häkkinen, W. Abbet, A. Sanchez, U. Heiz, U. Landman, *Angew. Chem. Int. Ed.* 42 (2003) 1297.
- [6] B. Yoon, H. Häkkinen, U. Landman, A.S. Worz, J.M. Antonietti, S. Abbet, K. Judai, U. Heiz, *Science* 307 (2005) 403.
- [7] S. Lee, C. Fan, T. Wu, S.L. Anderson, *J. Am. Chem. Soc.* 126 (2004) 5682.
- [8] B.E. Salisbury, W.T. Wallace, R.L. Whetten, *Chem. Phys.* 262 (2000) 131.
- [9] W.T. Wallace, R.L. Whetten, *J. Am. Chem. Soc.* 124 (2002) 7499.
- [10] Y.D. Kim, M. Fisher, G. Ganteför, *Chem. Phys. Lett.* 377 (2003) 170.
- [11] L.D. Socaciu, J. Hagen, T.M. Bernhardt, L. Wöste, U. Heiz, H. Häkkinen, U. Landman, *J. Am. Chem. Soc.* 125 (2003) 10437.
- [12] G. Mills, M.S. Gordon, H. Metiu, *Chem. Phys. Lett.* 359 (2002) 493.
- [13] N. Lopez, J.K. Nørskov, *J. Am. Chem. Soc.* 124 (2002) 11262.
- [14] X. Wu, L. Senapati, S.K. Nayak, A. Selloni, M. Hajaligol, *J. Chem. Phys.* 117 (2002) 4010.
- [15] B. Yoon, H. Häkkinen, U. Landman, *J. Phys. Chem. A* 107 (2003) 4066.
- [16] D.W. Yuan, Z. Zeng, *J. Chem. Phys.* 120 (2004) 6574.
- [17] X. Ding, Z. Li, J. Yang, J.G. Hou, Q. Zhu, *J. Chem. Phys.* 120 (2004) 9594.
- [18] E.M. Fernández, J.M. Soler, I.L. Garzón, L.C. Balbás, *Phys. Rev. B* 70 (2004) 165403.
- [19] J. Li, X. Li, H.J. Zhai, L.S. Wang, *Science* 299 (2003) 864.
- [20] H.F. Zhang, M. Stender, R. Zhang, C. Wang, J. Li, L.S. Wang, *J. Phys. Chem. B* 108 (2004) 12259.
- [21] A. Vittadini, A. Selloni, *J. Chem. Phys.* 117 (2002) 353.
- [22] C. Di Valentin, L. Giordano, G. Pacchioni, N. Rösch, *Surf. Sci.* 522 (2003) 175.
- [23] A. Del Vito, L. Giordano, G. Pacchioni, N. Rösch, *Surf. Sci.* 575 (2005) 103.
- [24] <http://www.fysik.dtu.dk/CAMPOS>.
- [25] M.C. Payne, M.P. Teter, D.C. Allan, T.A. Arias, J.D. Joannopoulos, *Rev. Mod. Phys.* 64 (1992) 1045.
- [26] D. Vanderbilt, *Phys. Rev. B* 41 (1990) R7892.
- [27] J.P. Perdew, et al., *Phys. Rev. B* 46 (1992) 6671.
- [28] L. Xiao, L. Wang, *Chem. Phys. Lett.* 392 (2004) 452.
- [29] H. Häkkinen, M. Moseler, U. Landman, *Phys. Rev. Lett.* 89 (2002) 033401.
- [30] F. Furche, R. Ahlrichs, P. Weis, C. Jacob, S. Gilb, T. Bierweiler, M.M. Kappes, *J. Chem. Phys.* 117 (2002) 6982.
- [31] N. Lopez, T.V.W. Janssens, B.S. Clausen, Y. Xu, M. Mavrikakis, T. Bligaard, J.K. Nørskov, *J. Catal.* 223 (2004) 232.
- [32] L.M. Molina, B. Hammer, *Phys. Rev. B* 69 (2004) 155424.
- [33] P. Broqvist, L.M. Molina, H. Grönbeck, B. Hammer, *J. Catal.* 227 (2004) 217.
- [34] M.P. Johansson, D. Sundholm, J. Vaara, *Angew. Chem. Int. Ed.* 43 (2004) 2678.
- [35] W.T. Wallace, R.L. Whetten, *J. Phys. Chem. B* 104 (2000) 10964.
- [36] H.-J. Zhai, L.-S. Wang, *J. Chem. Phys.* 122 (2005) 051101.